AD-A166 332 PATHS AND IONIZATION LOSSES OF PROTON ENERGY IN DIFFERENT SUBSTANCES(U) FOREIGN TECHNOLOGY DIV WRIGHT-PATTERSON AFB OH I M VASILOVSKIY ET AL. 1/1

UNCLASSIFIED 14 FEB 86 FTD-ID(RS)T-1507-84 F/G 20/8 NL

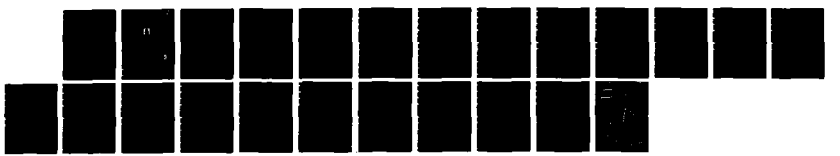

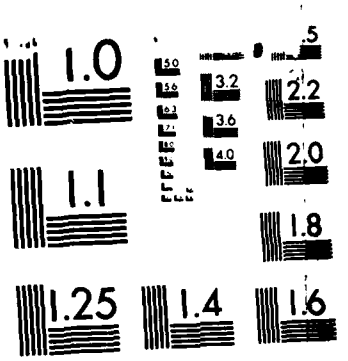

FTD-ID(RS)T-1507-84

# FOREIGN TECHNOLOGY DIVISION


PATHS AND IONIZATION LOSSES OF PROTON ENERGY IN DIFFERENT SUBSTANCES

by

I.M. Vasilovskiy, I.I. Karpov, et al.


DTIC
ELECTE
APR 03 1986
S D
E

AD-A166 332

DTIC FILE COPY

Approved for public release;
distribution unlimited.

# EDITED TRANSLATION

FTD-ID(RS)T-1507-84 14 February 1986

MICROFICHE NR: FTD-86-C-001503

PATHS AND IONIZATION LOSSES OF PROTON ENERGY IN DIFFERENT SUBSTANCES

By: I. M. Vasilovskiy, I. I. Karpov, et al.

English pages: 19

Source: Probegi i Ionizatsionnyye Poteri Energii Protonov v Razlichnykh Veshchestvakh, P1-4081, 1968, pp. 1-27

Country of origin: USSR
Translated by: Robert D. Hill
Requester: AFWL/IN
Approved for public release; distribution unlimited.

## U. S. BOARD ON GEOGRAPHIC NAMES TRANSLITERATION SYSTEM

| Block | Italic | Transliteration | Block | Italic | Transliteration |
|---|---|---|---|---|---|
| А а | *А а* | A, a | Р р | *Р р* | R, r |
| Б б | *Б б* | B, b | С с | *С с* | S, s |
| В в | *В в* | V, v | Т т | *Т т* | T, t |
| Г г | *Г г* | G, g | У у | *У у* | U, u |
| Д д | *Д д* | D, d | Ф ф | *Ф ф* | F, f |
| Е е | *Е е* | Ye, ye; E, e* | Х х | *Х х* | Kh, kh |
| Ж ж | *Ж ж* | Zh, zh | Ц ц | *Ц ц* | Ts, ts |
| З з | *З з* | Z, z | Ч ч | *Ч ч* | Ch, ch |
| И и | *И и* | I, i | Ш ш | *Ш ш* | Sh, sh |
| Й й | *Й й* | Y, y | Щ щ | *Щ щ* | Shch, shch |
| К к | *К к* | K, k | Ъ ъ | *Ъ ъ* | " |
| Л л | *Л л* | L, l | Ы ы | *Ы ы* | Y, y |
| М м | *М м* | M, m | Ь ь | *Ь ь* | ' |
| Н н | *Н н* | N, n | Э э | *Э э* | E, e |
| О о | *О о* | O, o | Ю ю | *Ю ю* | Yu, yu |
| П п | *П п* | P, p | Я я | *Я я* | Ya, ya |

*ye initially, after vowels, and after ъ, ь; e elsewhere.
When written as ё in Russian, transliterate as yё or ё.

## RUSSIAN AND ENGLISH TRIGONOMETRIC FUNCTIONS

| Russian | English | Russian | English | Russian | English |
|---|---|---|---|---|---|
| sin | sin | sh | sinh | arc sh | $\sinh^{-1}$ |
| cos | cos | ch | cosh | arc ch | $\cosh^{-1}$ |
| tg | tan | th | tanh | arc th | $\tanh^{-1}$ |
| ctg | cot | cth | coth | arc cth | $\coth^{-1}$ |
| sec | sec | sch | sech | arc sch | $\operatorname{sech}^{-1}$ |
| cosec | csc | csch | csch | arc csch | $\operatorname{csch}^{-1}$ |

| Russian | English |
|---|---|
| rot | curl |
| lg | log |

## GRAPHICS DISCLAIMER

**All figures, graphics, tables, equations, etc. merged into this translation were extracted from the best quality copy available.**

# PATHS AND IONIZATION LOSSES OF PROTON ENERGY IN DIFFERENT SUBSTANCES

I.M. Vasilovskiy, I. I. Karpov, V. I. Petrukhin, Yu. D. Prokoshkin

## 1. Introduction.

Ionization energy losses of charged particles in a substance are described by the well-known Bethe-Bloch formula,

$$-\frac{dE}{ds} = F(\beta)\left[ f(\beta) - \ln I - \sum_{K,L,\ldots} C_i - \frac{\delta}{2} \right]. \qquad (1)$$

However, if in this formula we use corrections $C_1$, which consider the connection of the electrons only on the K and L shells of the atoms [1], then magnitudes of the ionization potentials $I$ (which, by definition, must not depend on the velocity of the particle $\beta$) in region of low proton energies ($E < 100$ MeV) for heavy elements prove to be considerably larger than those at high energies [2, 3, 4]. The calculation of corrections of $\delta$, which are connected with the effect of density, does not change this deduction, since at energies $E < 700$ MeV magnitudes of $\delta$ are insignificant [5].

In the high energy region corrections $C_1$ are small, and the error in their determination has little effect on the accuracy of measurement of the ionization potentials. When the energy E is decreased, the corrections $C_1$ are rapidly increased, and together with $C_K$ and $C_L$ a substantial role should be played by corrections for the higher electron orbits ($C_M$, $C_N$ ...). To determine these corrections (the theoretical data about which are as yet absent) a semiempirical procedure [6, 7] was proposed: by analogy with $C_K$ and $C_L$ the total correction C is approximated by the polynomial

$$C = \sum_{K,L,\ldots} C_i = \sum a_i \eta^{-2i} . \qquad (2)$$

where $\eta^2 = \beta^2/(1-\beta^2)$. Coefficients $a_j$ are selected so that formula (1) would describe well the experimental data with ionization potentials I not dependent on energy [7]. This procedure is equivalent to the fact that values of I are found from data obtained at high energies, and for low energies, on the basis of relation (1) and experimental data on ionization energy losses and paths, the corrections C are determined. Thus studies of ionization losses in the region of high energies are the main source of the experimental information necessary for the correction of relation (1), and determination of magnitudes of ionization potentials I.

The purpose of this work was to measure the magnitudes of ionization losses dE/ds, paths R and ionization potentials I at a proton energy of E 670 MeV. The measurements were taken by the relative method for different substances of x, and the magnitudes of $q_x=(dE/ds)_x/(dE/ds)_{Al}$ and $\rho_x=R_x/R_{Al}$ were found. Quantities $q_x$ and $\rho_x$ weakly depend on the energy E:

$$q_x(E+\Delta E)=q_x(E)\left(1+a\frac{\Delta E}{E}\right), \qquad (3)$$

where at E=200-600 MeV, $a=(2-4)\cdot 10^{-2}$ for different substances. The proton energy was determined with an accuracy of 2 MeV. This error in the measurement of E corresponds to the indeterminancy in $q_x$, equal to $(0.5-4)\cdot 10^{-4}$, which is less than the error of measurements of $q_x$ by an order of magnitude.

Measurements of $q_x$ and $\rho_x$ make it possible to determine the magnitudes of relative ionization potentials $I'_x=I_x/I_{Al}$ and, after normalization, the known value of $I_{Al}$, and to find the ionozation potentials of different substances $I_x$. Magnitudes of $I'_x$ weakly depend on $I_{Al}$:

$$I'_x(I_{Al}+\Delta I_{Al})=I'_x(I_{Al})\left(1+b\frac{\Delta I_{Al}}{I_{Al}}\right), \qquad (4)$$

where b=1/15. The indeterminancy of quantity $I_{Al}$ does not exceed 2%. This corresponds to a determination error of $I'_x$ equal to $1.5\cdot 10^{-3}$, which is less than the experimental error of $I'_x$ by an order of magnitude.

2. Procedure of measurements.

Measurements of paths and ionization losses of proton energy for Al, Cu, Sn, and Pb were taken on the derived proton beam of the

synchrocyclotron of the Laboratory of Nuclear Problems of OIYaI [Joint Institute of Nuclear Research]. The proton beam was shaped by means of a deflecting magnet and a system of collimators. Characteristics of the beam were investigated earlier by the method of the magnetic sprectrometer [8]. The distribution of protons with respect to energy E is described by the Gaussian curve with the standard

$$\Delta_E = (2{,}8 \pm 0{,}3) \text{ MeV} \qquad (5)$$

The mean energy of the protons in the beam depended on conditions of the beam extraction from the synchrocyclotron and was measured within limits of 660 to 670 MeV.

Paths of protons in different substances were determined by the method of the Bragg curve. A diagram of the experiment is given on Fig. 1. Placed into the proton beam were two thin-walled ionization chambers 8 cm in diameter, IK1 and IK2, and located between these were the main filter F of the substance being studied and an additional wedge-like filter. Placed behind the ionization chamber IK2 was a small mobile scintilllation counter C, which operated in the integral mode. The profile of the beam was determined by this counter, and its adjustment was made with an accuracy better than 1 mm. The current of the ionization chambers was measured by means of electrometrical amplifiers EMU-1 and recorded by recording potentiometers EPP-09. To avoid pickups, the ionization chambers and transmission channels and feed channels were carefully screened. The power feed of the chambers was accomplished from shielded galvanic elements.

The first chamber IK1 measured the intensity of the proton beam going to the filter, and determined by chamber IK2 was the Bragg curve B(s) - the dependence of the current of the ionization chamber on the thickness of the suppressor filter s. In the process of measurements, the thickness s was measured (by means of movement of the wedge) synchronously with movement of the tape of the potentiometer, on which a continuous recording of the Bragg curve was made. At the same time of the recording of the Bragg curve, datum marks, which correspond to the recorded values of the wedge's thickness, were applied to the tape. The standard Bragg curve is given on Fig. 2.

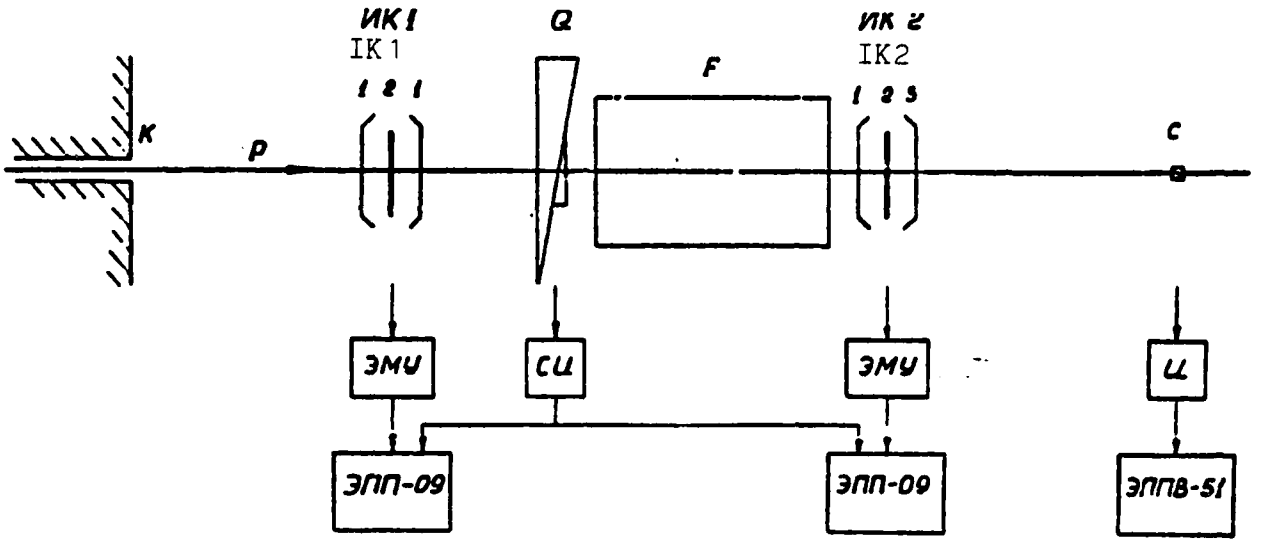


Fig. 1. Diagram of the experiment. P - proton beam, K - output collimator, IK1 and IK2 - ionization chambers, 1 - high-voltage electrode, 2 - signal electrode, 3 - remote movable electrode, Q - wedge-like electrode, F - main filter, C - scintillation counter, EMU[ЭМУ] - electrometric amplifier, SI [СИ] - system of precise display of position of wedge, I[И] - integrator, EPP[ЭППП] - recording potentiometer.

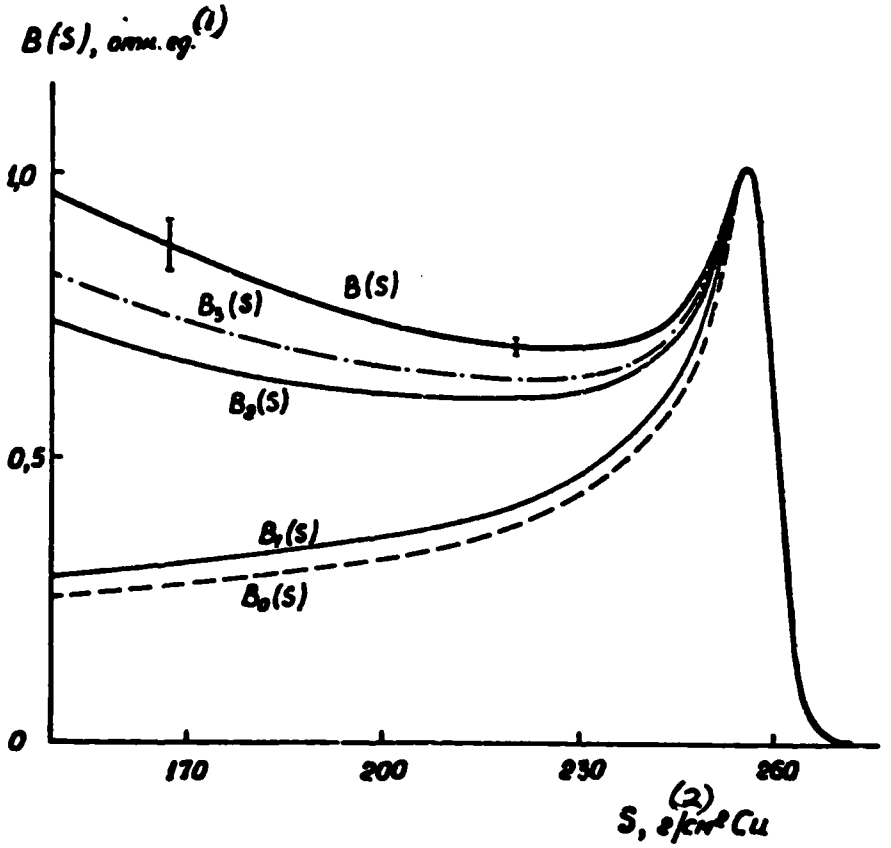


Fig. 2. Bragg curve for protons in copper when E=660 MeV. Distance

between filter F and central electrode of chamber IK2 =8 cm. B(s) - results of measurements. Calculation curves successively consider [9]: scattering of beam protons with respect to energy and fluctuation of losses of energy ($B_0$), multiple Coulomb scattering ($B_1$), nuclear interaction ($B_2$), and meson formation ($B_3$). Key: (1) relative units; (2) $g/cm^2$.

Two wedge-like filters, aluminum and copper, were used in measurements of the paths R. The main filters F were made of graphite, aluminum, copper, and lead. The thickness of the filters s (in $g/cm^2$) was determined by the weighing and measuring of dimensions of the specimens with an accuracy better than $5 \cdot 10^{-4}$. Measurements of Bragg curves for each substance were repeated with several sets of specimens making up the filter F. The obtained values of the paths coincide within limits of errors of the measurements. To increase the accuracy of determination of the relative paths, the recording of the functions B(s) was repeated again and again in each series of measurements for all the substances studied.

In the measurement of the relative suppressor capacities $q_x$, quantity R for aluminum was determined; then one of the specimens of the aluminum filter F was replaced by the specimen of the substance x being investigated, and again the quantity R was measured. This operation was repeated agin and again, and the thickness of the specimens was equivalent in suppressor capacity to 30 $g/cm^2$ of Al.

To raise the accuracy of the measurements, the differential operating mode of the ionization chamber IK2 was used: measured was the difference of currents in the first and second parts of the chamber separated by the central electrode with a thickness of 1.2 $g/cm^2$ Cu. Here, unlike the standard mode, voltage of the opposite sign was applied to the two external high-voltage electrodes of the chamber. Adjustment of the differential mode (compensation of currents in the first and second parts of the chamber) was carried out by changing the distance between the central and second high-voltage electrodes of the chamber. The standard differential Bragg curve B'(s) is given on Fig. 3. Use of the differential ionization chamber, together with the increase in accuracy and speed of the measurements, also makes it possible to check the energy spectrum of the proton

beam. The energy resolution of the differential chamber is sufficient to reveal the impurity of the protons,* the energy of which differs from the energy of the main beam by several MeV (Fig. 4). [Footnote* As the experiments in Berkley showed [11], the derived beam can contain an impurity of low-energy protons.]

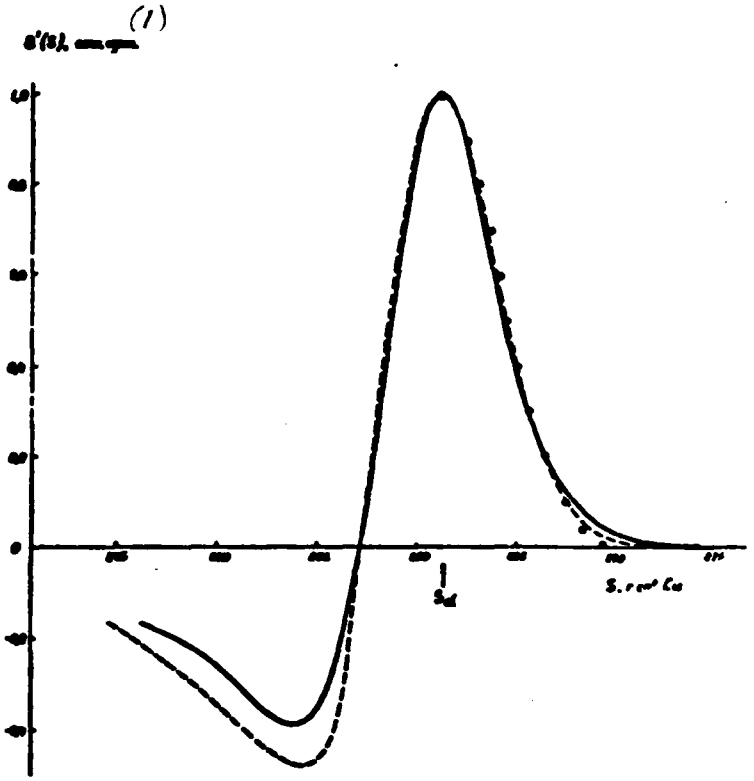


Fig. 3. Differential Bragg curve B'(s) for protons in copper when E=660 MeV and =8 cm. Solid curve - results of the measurements, dashed curve is calculated by the Monte Carlo method [9]; circles - Gaussian function with the standard (7) approximating the calculation curve B'(s). Key: (1) relative units.

3. Shape of Bragg curves.

Magnitudes of paths R were determined by comparing the measured Bragg curves and dependences B(s) computed by using formula (1). The calculation of dependences B(s) was done by the Monte Carlo method, which considers the fluctuations of losses of energy, the scattering of particles with respect to energy and repeated Coulomb scattering and the nuclear interaction of the particles [9]. Since the effects of scattering depend on the geometry of the experiment, calculations

of B(s) were made for the same specific conditions in which measurements of the paths and ionization energy losses were taken.

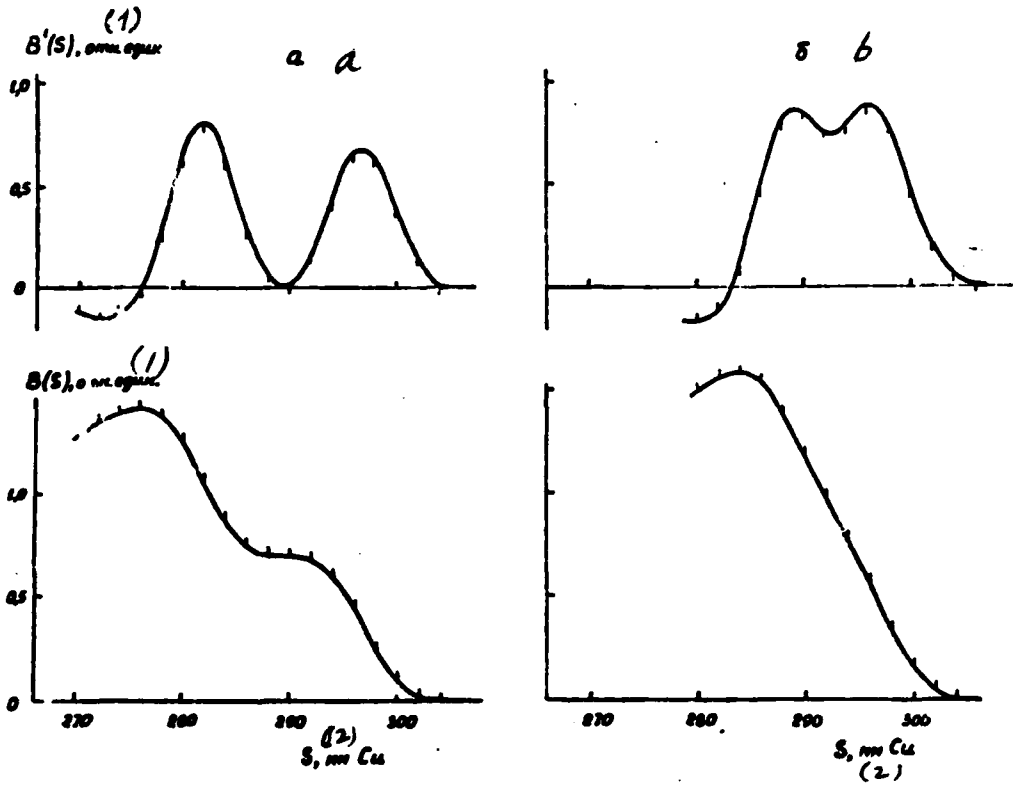


Fig. 4. Resolution of the differential ionization chamber. B(s) and B'(s) - Bragg curves and differential Bragg curves measured for protons in copper. Part of the proton beam is covered by a polyethylene filter, in which the initial proton energy E=660 MeV is decreased by 23 MeV (a) and 11 MeV (b). The distance between the datum marks is 2 mm Cu. Key: (1) relative units; (2) mm.

The scattering of the protons along paths caused by fluctuations of energy losses is described by the Gaussian curve with sufficient accuracy. The standard of this curve $\sigma_{CT}$ was calculated by Sternheimer for different substances [10]. Since the scattering along the paths, which is connected with the initial scattering of the proton beam with respect to energy (5), is also well described by the Gaussian curve [8], then the resulting distribution of protons along the paths can be represented by the Gaussian curve with the standard

$$\sigma = (\sigma_{CT}^2 + \sigma_E^2)^{1/2}, \qquad (6)$$

where $\sigma_E = \Delta_E (dE/ds)^{-1}$.

Calculations of functions B(s) were made for a number of values of at different distances of $\ell$ between the filter F and central electrode of the chamber IK2. Figure 5 gives results of the calculation for copper with the path of the protons of $R_{Cu}$=260 g/cm$^2$ and $\ell$=4 cm. As is evident from the figure, when the scattering and nuclear interaction of the suppressing protons are not considered, function B(s) virtually does not depend on $\sigma$ in the vicinity of point $s_0$=0.9997 $R_{Cu}$. This value of s corresponds to $B(s_0)$=0.792 $B(s)_{max}$,* where $B(s)_{max}$ is the value of the Bragg curve in the maximum (see Fig. 2). [Footnote*: The values of $s_0$ and $B(s_c)$ differ a little from those computed by Maser and Segre, who use the approximation function dE/ds(s) in the calculations.] If we consider the scattering and nuclear interaction of the protons, the intersection point of the curves $s_0$ is shifted to the region of large paths. This shift weakly depends on $\ell$. Quantity $B(s_0)$ with [word illegible] $\ell$ is little changed. When $\ell$ > 10 cm, $B(s_0)$ is rapidly decreased with an increase in $\ell$. A similar result is obtained for other substances.

In a comparison the forms of the measured and computed functions of B(s) were normalized to unity in the maximum $B(s)_{max}$ and were combined in scale s at point $s_0$. At the same time, quantity $\sigma$ was varied (formula (6)). The value of $\sigma$ (from the least-square method) from copper was found equal to $\sigma$ =(3.06+0.09) g/cm$^2$ Cu when [?]=260 g/cm$^2$. The calculation value of $\sigma_{c\tau}$ [10] was used, and hence we obtain $\Delta_E$=(2.8+0.3) MeV, which concurs with data of the direct measurments (5). The computed and measured Bragg curves agree well with each other when s ≥ R (Fig. 2). In the region up to the maximum there is observed the difference between the curves, which is connected, possibly, with the approximation nature of the calculation [9].

The following procedure was taken in determining the paths according to the Bragg curves: the value of $s'_0$ corresponding to $B(s_0)$=0.79 $B(s)_{max}$, and then there were introduced calculation corrections which consider the initial shift of $\Delta s_0$ of point $s'_0$ with respect to s=R, taking into account the scattering and nuclear interaction of the protons) and the shift due to the scattering ($\Delta s_1$) and nuclear interaction ($\Delta s_2$) in cm.

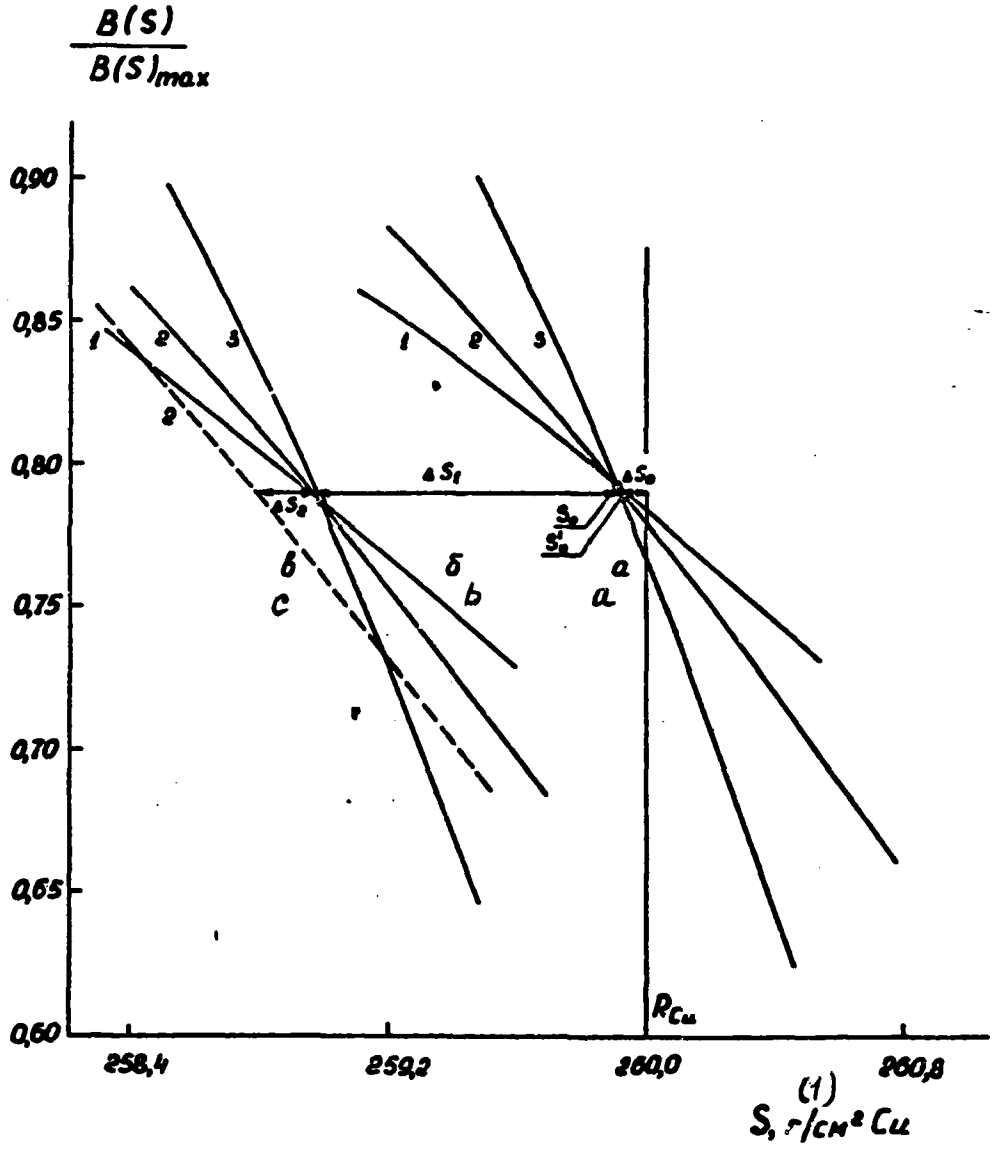


Fig. 5. Shape of the Bragg curve B(s) in the vicinity of point $s_0$ for protons in copper when E=660 MeV and $\ell$ =4 cm. 1, 2, 3 - $\sigma$ =4.59, 3.06 and 1.53 g/cm$^2$ Cu, respectively. a - calculated without taking into account the Coulomb scattering and nuclear interaction of protons, b - taking Coulomb scattering into account, c - taking into account the Coulomb scattering and nuclear interaction.
Key: (1) g/cm$^2$.

5. When $R_{Cu}$=260 g/cm$^2$ and $\ell$ =8 cm, these corrections are equal to 0.03%, 0.47% and 0.07%, respectively; the total correction of $\delta R = \Delta s_0 + \Delta s_1 + \Delta s_2$ to the path measured at point $s'_0$ is 0.57%. It should be noted that in the measurement of the relative quantities $q_x$ and $p_x$, the precise selection of [word illegible] and determination of the path on the Bragg curve is not as significant as that in the measurement of paths $R_x$, since the replacement of one substance by its form of the Bragg curve in the vicinity of $s'_0$ is insignificantly changed.

Differential curves of Bragg B'(s) were computed by the method similar to that described earlier (let us note that $B'(s) \neq dB(s)/ds$ because of the scattering and nuclear interaction of the protons). The calculation values of B'(s) agree with the measured curves when $s \geqslant R$ (Fig. 3). Differences in the curves in the region $s < R$ can be explained both by the inaccuracy of the calculations and by the insufficiently compensated mode of the differential chamber.

In the region beyond the maximum, cuves B'(s) can be approximated by the Gaussian function with standard $\sigma_{диф}$ (Fig. 3), which at values of $\sigma$ close to (6) is proportional to $\sigma$:

$$\sigma_{диф} = k\sigma, \qquad (7)$$

and the quantity k is close to unity (for copper k=0.91). The use of relation (7) makes it possible to determine the quantity $\sigma$ on the basis of measurements of the differential Bragg curve. For copper, when $R_{Cu}$=260 g/cm$^2$, $\sigma$ =(3.0±0.1) g/cm$^2$ Cu, which agrees with the value computed from formula (6). The position of the maximum $s_d$ of curve B'(s) also depends on the quantity $\sigma$; however, this dependence is weak: with an increase in $\sigma$ of 3% (i.e., within limits of the accuracy of the experimental determination), the quantity $s_d$ is increased by 0.015%.

4. Paths of the protons.

To determine the paths of $R_x$ and relative paths of $p_x$, several series of measurements of Bragg curves were carried out. During the experiment, which lasted for about two years, the operating mode of the synchrocyclotron was repeatedly retuned, which resulted in a change in the energy of the derived beam E. The magnitude of E in

each series of measurements was determined from the proton path in aluminum; furthermore, it was monitored with an accuracy of 0.05 MeV on the position of the maximum of $s_d$ by the differential Bragg curve, which was repeatedly measured during a series of measurements.

In the first series of measurements the magnitude of $s'_0$ for Al was obtained equal to (224±70±0.07) g/cm$^2$ Al. The correction to the measured path $s'_0$ is equal to $\delta R$=(0.88±0.08) g/cm$^2$ Al. Hence $R_{Al}$=(225.4±0.1) g/cm$^2$. Using $I_{Al}$=(160±3) eV, we obtain E=(660±2) MeV. The indicated error of E is determined mainly by the error of measurement of $I_{Al}$. In the subsequent series of measurements, the quantity E varied from series to series within 660 to 670 MeV. For convenience of comparison, the obtained magnitudes of $p_x$ and $q_x$ are given below for one value of energy at the input to the wedge-like filter E=660 MeV.

Simultaneously with $R_{Al}$, the proton path in copper $R_{Cu}$ was measured (with the use of a copper wedge). A comparison of the obtained magnitude of $R_{Cu}$ with results of preceding measurements [4], where simultaneously with the path of $R_{Cu}$ the proton pulse was determined, showed that E=(660±1) MeV. The ratio $1p'_{Cu}$ of measured paths in aluminum and copper (without taking corrections of $\delta R$ into account) proved to be equal to 0.865±0.002. The magnitude of $p_{Cu}$ was measured also by the relative method with the use of the aluminum wedge (aluminum filter F was replaced by copper, and values of R were compared). In this case the proton energy at the inlet into the filter F consisted of E=625 MeV. The obtained value of $p_{Cu}$ by the relative method (see Table 1) agreed with the value found by comparing the total paths. Measurements of the relative paths $p_x$ were made also for graphite and lead (Table 1).

[See Table 1 on next page]

Table 1.

Relative paths of protons when E=625 MeV.

| X | $1/\rho_x$ | поправка, % (1) | $1/\rho_x$ | $I/\rho_x$ /II/ |
|---|---|---|---|---|
| C | I,II8±0,002 | 0,II±0,0I | I,II9±0,002 | |
| Al | I | 0 | I | I |
| Cu | 0,867±0,002 | -0,27±0,02 | 0,865±0,002 | 0,866 |
| Pb | 0,656±0,002 | -0,94±0,I0 | 0,650±0,002 | 0,654 |

Key: (1) correction, %.

At small $\ell$ the shape of the Bragg curve was virtually unchanged with replacement of one substance of filter F by another. Thus, the difference in magnitudes of $R_x$, determined by comparing the Bragg curves at points 0.79 $B(s)_{max}$ and 0.82 $B(s)_{max}$, when $\ell$ =8 cm consisted of a total of $(2-5)\cdot 10^4$. With an increase in $\ell$ the effects of the scattering become significant, and the difference is increased; when $\ell$ =30 for $p_{Cu}$ it is equal to $3\cdot 10^{-3}$.

5. Ionization energy losses.

Measurements of relative ionization losses of energy $q_x$ were taken for four different positions of the exchanged specimen inside the aluminum filter F. Effective values of energy $\hat{E}_{эфф}$ corresponding to these positions were determined as $E_{эфф}=0.6(E_1-E_2)+E_2$, where $E_1$ and $E_2$ are proton energies at the input and output from the adjacent specimen. The obtained values of relative losses of $q'_x$ (without taking corrections for scattering of $q_x$ into account) and $q_x$ are given in Table 2. Check measurements were also made for the quantity $q_{Cu}$, when $E_{эфф}$ =600 MeV, when a copper filter F and copper wedge werew used, and a replacement of the copper specimen in filter F by an aluminum specimen was made. The difference in the values of $q_{Cu}$ measured by the two methods was found equal to 0.0001±0.002.

[See Table 2 on next page.]

Table 2. Relative Ionization Energy Losses

$$q_x=(dE/ds)_x/(dE/ds)_{Al}$$

| $E_{эфф.}$, Мэв (1) | 110 | 300 | 420 | 600 |
|---|---|---|---|---|
| $I_c$ | I,I27±0,003 | I,II8±0,003 | I,II6±0,003 | I,II4±0,002 |
| $q_c$, % | 0,22 ±0,03 | 0,I6 ±0,02 | 0,II ±0,02 | 0,05 ±0,0I |
| $c$ | I,29 ±0,003 | I,I20±0,003 | I,II7±0,003 | I,II5±0,002 |
| $I'_{c_2}$ | 0,858±0,003 | 0,872±0,004 | 0,87I±0,003 | 0,873±0,002 |
| $c_2$, % | -0,67 ±0,I5 | -0,48 ±0,07 | -0,32 ±0,04 | -0,I3±0,02 |
| $I_{c_2}$ | 0,852±0,004 | 0,868±0,004 | 0,868±0,003 | 0,872±0,002 |
| $I'_{a_2}$ | 0,780±0,004 | 0,752±0,003 | 0,757±0,003 | 0,754±0,003 |
| $L_{a_2}$, % | -I,2 ±0,3 | -0,9 ±0,2 | -0,6 ±0,I | -0,20 ±0,04 |
| $a_2$ | 0,72I±0,005 | 0,745±0,004 | 0,752±0,004 | 0,758±0,003 |
| $I'_{Pb}$ | 0,687±0,003 | 0,659±0,003 | 0,66I±0,003 | 0,667±0,003 |
| $P_{Pb}$, % | -I,7 ±0,8 | -I,3 ±0,2 | -0,9 ±0,2 | -0,26 ±0,03 |
| $I_{Pb}$ | 0,626±0,005 | 0,65I±0,004 | 0,655±0,004 | 0,665±0,003 |

Key: (1) MeV.

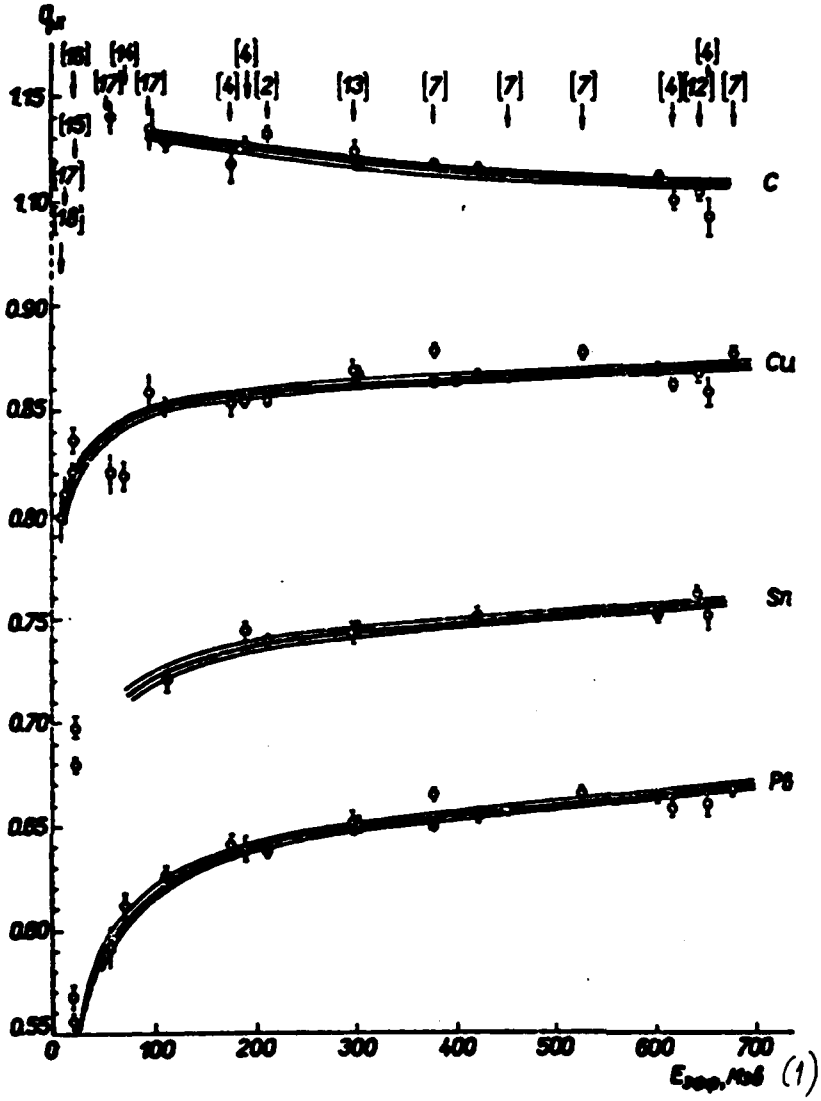


Fig. 6. Relative braking capabilities $q_x=(dE/ds)_x/(dE/ds)_{Al}$. The circles show results of measurement of $q_x$, the squares - $1/\rho_o$ with the appropriate effective energy $E_{эфф}$ and dark points - data of this work. Results of other works are indicated by brackets. Magnitudes of $q_x$, obtained on beams of deuterons and particles, are given in the equivalent energy of protons. Introduced into the data of Bakker and Segre [13] is the correction for the multiple Coulomb scattering. Values of $q_{Cu}$ and $q_{Pb}$, when E=20 MeV, are computed from data with $q_{Cd}$ and $q_{Cu}$. [Words are illegible] that 1=s. The curves show results of [words illegible] according to formula (1) with the use of corrections (2) of values [?] of potentials, are given in Table 3 [?]. The [words illegible] show the corridor of errors which correspond to [words illegible] determination of the relative ionization potentials $I'_x$.

Figure 6 gives values of $q_x$ found in this work jointly with data of preceding measurements. Given here are the obtained values of $\rho_x$ with values of effective energy $E_{эфф}=0.6\ E$ corresponding to them. As is evident from this figure, values of $q_{Cu}$ and $q_{Pb}$, obtained by the method of photoemulsion [11], exceed both the results of the remaining investigations and the values of $\rho_x$ measured in this work and are not decreased with energy E, as should be in conformity with (1). This divergence cannot be explained by the fact that in the work mentioned the correction $\delta q_x$ was not considered; it consists, by our extimate, of not more than 0.2% for copper and 0.4% for lead, and the introduction of it does not eliminate the difference.

6. Ionization Potential of Atoms

The obtained values of $\rho_x$ and $q_x$ were used for determining the relative ionization potentials $I'_x=I_x/I_{al}$. Potentials $I_x$ were found by normalizing the values of $I'_x$ on the value of the ionization potential of aluminum $I_{Al}=160$ eV. Values of $I'_x$ were determined by taking into account the corrections C introduced according to the semi-empirical formula (2) [7] and corrections $C_K$ and $C_L$ [1] (with replacement of $\beta^2$ by $\eta^2$ [6]).

The ionization potentials found from data on relative paths $\rho_x$ are given in Table 3. The errors pointed out in the table correspond to experimental errors of determination of $I'_x$, and we do not consider errors of measurements of $I_{Al}$ equal to 1-2%. As is evident from Table 3, the introduction of corrections $C_1$ changes little the values of the ionization potentials for carbon and copper. In the case of lead, this correction is significant: the decrease in the ionization potential connected with it exceeds the error of its measurement.

Magnitudes of ionization potentials, found from data on the relative losses of energy $q_x$ are given in Table 4. The relative ionization potentials $I'_x$, obtained in measurements of the paths and losses of energy, agree with each other and coincide within limits of the errors with results of the measurements taken by us earlier by the method of magnetic spectrometry [4] (Table 5). Table 5 gives values of potentials found by means of the averaging of results of measurements in the region of high energies ($E > 100$ MeV).

Table 3. Ionization Potentials Obtained from Data on Relative Paths x'

| Поправки (1) | С по ф-ле (2) [7] (2) | $C_2 + C_1$ [4,6] | Без поправок $C_1$ (3) |
|---|---|---|---|
| $I'_C$ | 0,515±0,008 | - | - |
| $I'_{Cu}$ | 2,02 ±0,04 | 2,03±0,04 | 2,04±0,04 |
| $I'_{Pb}$ | 5,20± 0,11 | 5,3 ±0,1 | 5,4 ±0,1 |
| $I_{C}$, эВ (4) | 82,4±1,3 | - | - |
| $I_{Al}$, эВ | 160 | 160 | 160 |
| $I_{Cu}$, эВ | 323± 6 | 324±6 | 326±6 |
| $I_{Pb}$, эВ | 831±18 | 839±18 | 856±18 |

Key; (1) Corrections; (2) from formula (2); (3) Without correction $C_1$.

The potential I as a function of the charge of nuclei of atoms of the braking substance is described by the empirical formula

$$I = s(10 + 5e^{-\frac{s}{10}}) \text{ eV} \qquad (8)$$

(see Fig. 7).

By using data of Table 5 on values of $I'_x$ and corrections (2), the dependences of $q_x$ on energy E were computed. As is evident from Fig. 6, these dependences describe well the experimental results.

In conclusion let us take this occasion to thank R. V. Bogdanov and D. A. Prokoshkin for their conducting of the chemical analysis of the substances used in this work.

[Tables 4 and 5 and Fig. 7 on next two pages.]

Table 4. Ionization Potentials Obtained from Data on the Relative Losses of Energy

| $E_{эфф}$, Мэв (1) | I′ (2) С попр. С по формуле (2)/7/ | I′ (3) С поправкой $C_K$ и $C_L$ /1,6/ | I′ (4) без поправок | $I_a$, эв (5) ($I_{Al}$ = 160 эв) (5) |
|---|---|---|---|---|
| 00 | 0,503±0,008 | - | - | |
| 20 | 0,504±0,0II | - | - | |
| 00 | 0,5I8±0,0I0 | - | - | |
| I0 | 0,5[illegible]±0,0I0 | 0,522±0,0I0 | 0,52I±0,0I0 | |
| (6) среднее | 0,5II±0,007 | | | 82±I |
| 00 | 2,02±0,04 | 2,02±0,04 | 2,03±0,04 | |
| 20 | I,99±0,05 | 2,00±0,05 | 2,00±0,05 | |
| 00 | I,94±0,07 | I,94±0,07 | I,95±0,07 | |
| I0 | 2,02±0,07 | 2,02±0,07 | 2,04±0,07 | |
| (6) среднее | 2,00±0,03 | | | 320±5 |
| 00 | 3,37±0,I0 | 3,38±0,I0 | 3,39±0,I0 | |
| 20 | 3,I7±0,II | 3,I8±0,II | 3,I9±0,II | |
| 00 | 3,23±0,I2 | 3,24±0,I2 | 3,26±0,I2 | |
| I0 | 3,37±0,I5 | 3,4I±0,I5 | 3,47±0,I5 | |
| (6) среднее | 3,28±0,09 | | | 525±I4 |
| 00 | 5,20±0,I6 | 5,28±0,I6 | 5,33±0,I6 | |
| 20 | 5,26±0,2I | 5,3[illegible]±0,2I | 5,42±0,2I | |
| 00 | 5,09±0,2[illegible] | 5,I5±0,20 | 5,27±0,2I | |
| I0 | 4,92±0,27 | 5,22±0,29 | 5,49±0,3I | |
| (6) среднее | 5,I6±0,I3 | | | 826±2I |

Key: (1) MeV; (2) corrections C from formula; (3) With correction; (4) without corrections; (5) eV; (6) average.

Table 5. Ionization Potentials from data Obtained at High Energies

| Метод (1) | $I'_C$ | $I'_{Al}$ | $I'_{Au}$ | $I'_{Pb}$ | $I_H$ [3] | $I_C$ | $I_{Al}$ | $I_{Au}$ (в эВ) | $I_{Au}$ | $I_{Pb}$ |
|---|---|---|---|---|---|---|---|---|---|---|
| (2) Кривая Брэгга (наст. работа) | 0,515±0,008 | 2,02±0,04 | - | 5,20±0,11 | | | | | | |
| (3) Кривая Брэгга (наст. работа) | 0,511±0,007 | 2,00±0,03 | 3,28±0,09 | 5,16±0,13 | | | | | | |
| Среднее (наст. работа) (4) | 0,513±0,006 | 2,01±0,03 | 3,28±0,09 | 5,18±0,10 | - | 82±1 | 160 | 322±5 | 525±14 | 880±17 |
| (5) Среднее из данных магн. спектр., кривая Брэгга | 0,535±0,020 | 2,06±0,03 | 3,2 ±0,1 | 5,2 ±0,2 | | | | | | |
| фотоэмульсия [11] (6) | - | 1,98±0,03 | - | 5,1 ±0,1 | | | | | | |
| Среднее (7) | 0,516±0,008 | 2,02±0,03 | 3,24±0,08 | 5,16±0,08 | 17 ±2 | 82,5±13 | 160 | 323±5 | 518±13 | 826±14 |
| $I'_i/(Z_i/Z_{Al})$ | | | | | 1,38±0,16 | 1,118±0,017 | 1 | 0,806±0,014 | 0,843±0,021 | 0,812±0,01 |
| $I/Z$ | | | | | 17 ± 2 | 13,8 ±0,2 | 12,3 | 11,1±0,2 | 10,4 ±0,2 | 10,1 ±0,2 |

Key: (1) Method; (2) Bragg curve (this work); (3) diffusion Bragg curve; (4) Average (this work); (5) Average data [3], magnetic spectrum, Bragg curve; (6) photoemulsion [11]; (7) average.

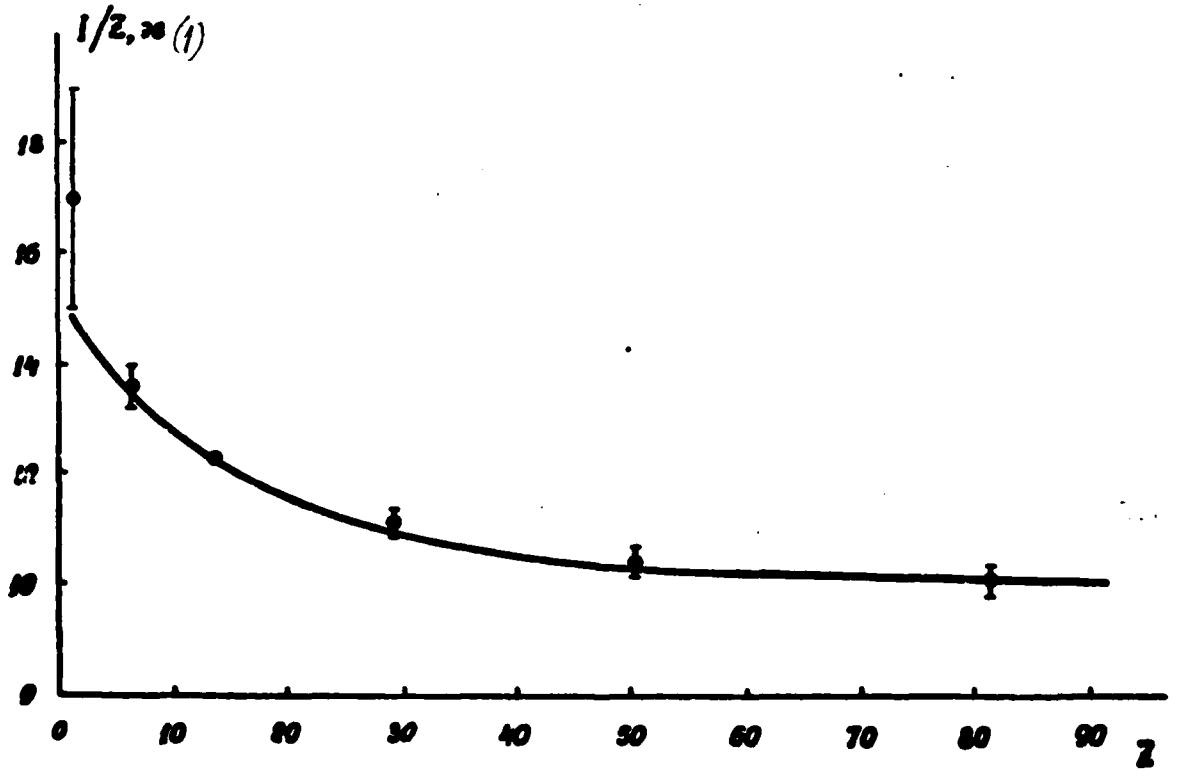


Fig. 7. x - dependence of ionization potential I. Curve - function (8), points - data of Table 5.

Manuscript received in publishing department on 20 September 1968.

References

1. M.C. Walske. Phys. Rev., 88, 1283 (1952); 101, 940 (1956).
2. R. Mather, E. Segre. Phys. Rev., 84, 191 (1951).
3. В.П.Зрелов, Г.Д.Столетов. ЖЭТФ, 36, 658 (1959).
4. И.М.Василевский, Ю.Д.Прокошкин. Препринт ОИЯИ, Д-866, Дубна, 1960; ЯФ, 4, 548 (1966).
5. R.M. Sternheimer. Phys. Rev., 88, 851 (1952); 91, 256(1953); 103, 511 (1956).
6. H. Bichsel. Univ. of South Calif. Tech. Rep. No.2,3 (1961).
7. W.H. Barkas, M.J. Berger, NAS-NRC, USA. Publ. 1133(1962).
8. И.М.Василевский, Ю.Д.Прокошкин. Атомная энергия, 7, 225 (1959).
9. И.М.Василевский, И.И.Карпов , Ю.Д.Прокошкин. Препринт ОИЯИ, Р-4000, Дубна, 1968.
10. R.M. Sternheimer. Phys. Rev., 117, 485 (1960).
11. W.H. Barkas, S. von Friesen. Suppl. Nuovo Cim., 19,41(1961).
12. В.Е.Алейников, И.М.Василевский. Дипломная работа ОИЯИ, 1966.
13. C.J. Bakker, E. Segre. Phys. Rev., 81, 489 (1951).
14. N. Bloembergen, R.J. van Heerden. Phys. Rev., 83, 561 (1951).
15. C.P. Sonett, K.R. MacKenzie. Phys. Rev., 100, 734(1955).
16. V.C. Burkig, K.R. MacKenzie. Phys. Rev., 106, 848 (1957).
17. Э.Сегре (ред.) Экспериментальная ядерная физика, 1, ч. II, 172, ИЛ., Москва, 1955.
18. E.L. Kelly. Phys. Rev., 75, 1006 (1949).

END

DTIC

5-86